Radiative Exchange Between Gray Fins Using a Coupled Integral Equation Formulation

J. I. Frankel* and T. P. Wang†
Florida Institute of Technology, Melbourne, Florida

This paper presents an analytic methodology for determining the temperature and radiosity distributions in a rectangular, gray fin array through a primitive formulation that explicitly couples the two distributions. The primitive formulation, used in conjunction with the Green's function method, produces a set of coupled nonlinear Fredholm integral equations for temperature and radiosity that must be solved simultaneously. Accurate numerical results are produced rapidly and efficiently using the trapezoidal method and a standard iterative scheme. Initially, an integro-differential equation is derived from the one-dimensional steady-state energy balance. This mixed mode equation displays the coupling between the temperature and radiosity. In deriving the energy balance, a temperature-dependent thermal conductivity is included in terms of a Taylor series expansion. The Green's function method is used to convert the integro-differential equation describing the conservation of energy into an equivalent integral equation. The second integral equation is developed from the balance of radiant energy for a diffuse-gray surface. The coupled integral equations are solved simultaneously by a simple numerical integration scheme. A parametric study considering the effects of the conduction-radiation number, emissivity, spacings, and thermal conductivity is presented.

Nomenclature

a	= distance between fins
b	= thickness of a fin
B	= dimensionless distance between fins, d/w
$f(\eta,\theta,Q_o)$	= function defined by Eq. (8c)
$G(\eta,\eta_o)$	= Green's function
$k(T)$	= temperature-dependent thermal conductivity
L	= linear differential operator defined by Eq. (8b)
$MMAX$	= maximum number of terms used in Taylor's series
N_r	= radiation-conduction number, $\varepsilon\sigma T^3 w^2/(k_o t)$
$q''_{c,x}(x)$	= heat flux associated with conduction at x
$q''_{r,i}(x)$	= irradiation
$q''_{r,o}(x)$	= radiosity
$Q_o(\eta)$	= dimensionless radiosity
t	= half thickness of rectangular fin, $t = b/2$
T_b	= base temperature
w	= length of a fin
x	= coordinate
x_1	= coordinate
β_m	= Taylor series coefficient
β^*_m	= dimensionless Taylor series coefficient
ε	= total hemispherical emissivity
η,η_o	= dimensionless spatial variables
$\theta(\eta)$	= dimensionless temperature
ξ	= dummy variable used in integrations
σ	= Stefan-Boltzmann constant
τ	= dimensionless ratio of t/w
ω	= under-relaxation constant

Introduction

In the past, investigators[1-5] have addressed the problem of radiant heat transfer in fin arrays. It is well known that this mode of heat transfer is important in space applications where no convecting medium exists. In these situations, radiative heat transfer represents the only mode in which waste heat may be dissipated. In this study, we shall reformulate the governing equations into a more conducive form for numerical approximation. Unlike the previous studies, no finite differences or finite elements are required in this new formulation. The proposed numerical procedure involves only numerical integration.

The conservation of energy in an opaque solid and the balance of radiant energy for a diffuse-gray surface are used in their fundamental forms. Analytic manipulations of the conservation of energy permit the conversion of the integro-differential equation into an equivalent Fredholm integral equation. This is the key step in the proposed analytic procedure. The present analysis also includes the effects of a temperature-dependent thermal conductivity in the form of a Taylor series expansion.[6]

The objective of this study is to demonstrate that the primitive (fundamental) formulation, used in conjunction with Green's functions, permits an accurate and rapid numerical scheme to be developed for conduction-radiation fin problems. The Green's function method permits the systematic and efficient conversion of the integro-differential equation governing the conservation of energy into a "pure" integral equation. Using this expression and the integral equation describing the balance of radiant energy, two nonlinear integral equations coupling the temperature and radiosity are in a convenient form for numerical approximation. This formulation requires only a simple numerical integration and iterative procedure. The analytic and numeric procedure will be described, and a detailed parametric study will be presented.

Problem Formulation

In the past, the usual formulation involving mixed mode heat transfer (specifically conduction-radiation) has led to an integro-differential equation in temperature.[7,8] Finite difference (FD) and finite element (FE) methods are usually applied in resolving the temperature distribution for this type of problem. In constrast, we shall demonstrate that the energy balance and balance of radiant energy used in their primitive form can lead to a viable solution without resorting to FD or FE methods. That is, by using analytic developments prior to initiating any numerical procedure, one can convert the governing equations into a more amenable form for numerical approximation. The resulting equations will only require numerical integration.

This paper considers the development and solution of two coupled integral equations from which the temperature and

Received May 7, 1987; revision received Oct. 28, 1987.

*Assistant Professor, Mechanical and Aerospace Engineering Department. Member AIAA.

†Graduate Student, Mechanical and Aerospace Engineering Department.

radiosity distributions may be resolved simultaneously. Figure 1 displays the physical problem to be resolved. This figure shows a rectangular fin array in which diffuse-gray surfaces are assumed.[7] The fins are attached to a common black isothermal base at temperature T_b. The gray fins are of equal length w and thickness $b = 2t$. These fins are spaced a apart and extend indefinitely in the z direction. For simplicity, the environment temperature is assumed to be at 0 K.

A one-dimensional model is chosen since the fins are assumed to be thin ($b \ll w$). Under this restriction, the temperature and radiosity distributions in each fin are only a function of the x direction. Furthermore, by symmetry, the variations in temperature and radiosity are identical in each fin for fixed x when the material and surface properties of each fin are the same. Therefore the desired expressions are developed by considering half-a-fin thickness, namely $b/2 = t$. Steady-state conditions are assumed throughout this analysis. (Transient analysis may be performed in a manner similar to that proposed in this paper, though a multidimensional integral equation will be produced.)

From considering a differential element of length $\mathrm{d}x$ per unit width of the fin, as shown in Fig. 1, one can derive the conservation of energy as

$$q''_{c,x}(x)t + q''_{r,i}(x)\,\mathrm{d}x = q''_{r,o}(x)\,\mathrm{d}x + q''_{c,x+\mathrm{d}x}(x)t \tag{1}$$

where $q''_{c,x}t$, $q''_{c,x+\mathrm{d}x}t$ represent the amount of energy per unit time and per unit length entering and leaving the differential element by conduction, respectively. The irradiation and radiosity terms are represented by $q''_{r,i}\,\mathrm{d}x$ and $q''_{r,o}\,\mathrm{d}x$, respectively. The double prime notation indicates per unit area, e.g., (W/m^2). The constitutive relation used to describe heat conduction is known as Fourier's law and is given as

$$q''_{c,x}(x) = -k(T)\frac{\mathrm{d}T}{\mathrm{d}x} \tag{2}$$

where T is the temperature at x, and $k(T)$ is a temperature-dependent thermal conductivity. Recently,[6] the thermal conductivity $k(T)$ has been expressed in terms of a Taylor series expansion:

$$k(T) = k_o \sum_{m=0}^{MMAX} \beta_m (T - T_o)^m \tag{3}$$

where $\beta_o \equiv 1$, and T_o is some reference temperature. In theory, this representation will be exact for a single phase material as $MMAX \to \infty$. In addition, this form of $k(T)$ lends itself to further analytic manipulations in the three orthogonal coordinate systems.[6]

Using the net-radiation method[7,8] for a diffuse-gray surface, one can show that the outgoing radiation (radiosity) may be written as

$$q''_{r,o}(x) = \varepsilon\sigma T^4(x) + (1-\varepsilon)q''_{r,i}(x) \tag{4a}$$

This term consists of surface emission and the reflection of incident radiation for the assumed diffuse-gray surfaces. The incident radiation emanates from the enclosure that consists of the base, adjacent fins, and the environment, since each fin is assumed to be nonconcave. Mathematically, we write[7]

$$q''_{r,i}(x)\,\mathrm{d}x = \int_{x_1=0}^{w} q''_{r,o}(x_1)\,\mathrm{d}F_{\mathrm{d}x_1-\mathrm{d}x}\,\mathrm{d}x_1 + a\sigma T_b^4 F_{a-\mathrm{d}x} \tag{4b}$$

or, upon using reciprocity,

$$q''_{r,i}(x) = \int_{x_1=0}^{w} q''_{r,o}(x_1)\,\mathrm{d}F_{\mathrm{d}x-\mathrm{d}x_1} + \sigma T_b^4 F_{\mathrm{d}x-a} \tag{4c}$$

The terms $\mathrm{d}F_{\mathrm{d}x-\mathrm{d}x_1}$ and $F_{\mathrm{d}x-a}$ represent the differential forms of the configuration factors and can be found in Ref. 7. Equations (1–4) contain all the necessary ingredients to resolve the temperature, radiosity, and irradiation distributions in each fin once the boundary conditions have been specified. By assuming symmetry in the fins, we again note $q''_{r,o}(x) = q''_{r,o}(x_1)$ when $x = x_1$.

Expanding the conduction term in a Taylor series about x, substituting the expression for the irradiation terms given in Eq. (4c), and incorporating the constitutive relation with the generalized thermal conductivity into Eq. (1), we get

$$k_o t\frac{\mathrm{d}^2T}{\mathrm{d}x^2} = -k_o t\sum_{m=1}^{MMAX}\frac{\beta_m}{(m+1)}\frac{\mathrm{d}^2}{\mathrm{d}x^2}(T-T_o)^{m+1} + q''_{r,o}(x) - \left[\int_{x_1=0}^{w} q''_{r,o}(x_1)\,\mathrm{d}F_{\mathrm{d}x-\mathrm{d}x_1} + \sigma T_b^4 F_{\mathrm{d}x-a}\right] \tag{5}$$

Notice that the nonlinear contributions associated with the thermal conductivity have been written in a form suggesting that integration with some test function may be analytically performed.

Finally, the boundary conditions are written as

$$T(x) = T_b, \qquad x = 0 \tag{6a}$$

and

$$-k_o\sum_{m=0}^{MMAX}\frac{\beta_m}{(m+1)}\frac{\mathrm{d}}{\mathrm{d}x}(T-T_o)^{m+1} = \varepsilon\sigma T^4(x), \quad x = w \tag{6b}$$

In the next section, we shall detail the development of the new dual integral formulation.

Analysis

In this section, we shall describe an alternative integral equation formulation for mixed mode heat transfer as applied to fin analysis. The following dimensionless variables are introduced:

$$\eta = \frac{x}{w} \tag{7a}$$

$$\xi = \frac{x_1}{w} \tag{7b}$$

$$B = \frac{a}{w} \tag{7c}$$

$$\tau = \frac{t}{w} \tag{7d}$$

$$\theta(\eta) = \frac{T(x)}{T_b} \tag{7e}$$

$$Q_o(\eta) = \frac{q''_{r,o}(x)}{\varepsilon\sigma T_b^4} \tag{7f}$$

into Eqs. (4–6), where the reference temperature is now assumed at 0 K. The radiation-conduction number N_r[1,2,7] is defined as

$$N_r \equiv \frac{\varepsilon\sigma T_b^3 w^2}{k_o t} \tag{7g}$$

Substituting the dimensionless quantities expressed in Eqs. (7) and the appropriate shape (view) factors[7] into the energy balance expressed in Eq. (5) yields the following dimensionless heat equation:

$$L[\theta(\eta)] = f(\eta,\theta,Q_o) \tag{8a}$$

where L is the linear differential operator

$$L \equiv \frac{\mathrm{d}^2}{\mathrm{d}\eta^2} \tag{8b}$$

and

$$f(\eta,\theta,Q_o) = -\sum_{m=1}^{MMAX} \frac{\beta_m^*}{(m+1)} \frac{d^2}{d\eta^2}\theta^{m+1}(\eta) + N_r\left[Q_o(\eta) - \frac{B^2}{2}\int_{\xi=0}^{1} \frac{Q_o(\xi)\,d\xi}{[B^2+(\xi-\eta)^2]^{3/2}} - \frac{1}{2\varepsilon}\left(1-\frac{\eta}{(B^2+\eta^2)^{1/2}}\right)\right] \tag{8c}$$

where $\beta_m^* = \beta_m T_b^m$. The dimensionless form of the balance of radiant energy becomes

$$Q_o(\eta) = \theta^4(\eta) + (1-\varepsilon)\left[\frac{B^2}{2}\int_{\xi=0}^{1} \frac{Q_o(\xi)\,d\xi}{[B^2+(\xi-\eta)^2]^{3/2}} + \frac{1}{2\varepsilon}\left(1-\frac{\eta}{(B^2+\eta^2)^{1/2}}\right)\right] \tag{9}$$

Finally, the dimensionless boundary conditions become

$$\theta(\eta) = 1, \qquad \eta = 0 \tag{10a}$$

and

$$\frac{d\theta(\eta)}{d\eta} = -\sum_{m=1}^{MMAX} \frac{\beta_m^*}{(m+1)} \frac{d}{d\eta}\theta^{m+1}(\eta) - \tau N_r \theta^4(\eta), \qquad \eta = 1, \tag{10b}$$

where it is our intention to treat the right-hand side of Eq. (10b) as an effective nonhomogeneity. If an insulated condition is imposed at $\eta = 1$, the right-hand side of Eq. (10b) would be zero.

Next, we formally convert Eq. (8a) into an equivalent integral equation:

$$\theta(\eta) = L^{-1}[f(\eta,\theta,Q_o)] \tag{11a}$$

where L^{-1} is the inverse operator associated with L such that $L^{-1}L = LL^{-1} = I$ and where I is the identity operator. When such an inverse exists, it will take the form of an integral operator. The kernel of the integral operator will become the Green's function[9-12] associated with L.

The formal starting point in the development of the Green's function method[9-12] is the application of Green's first formula over the domain of interest, namely

$$\int_{\eta_o=0}^{1} L_o[\theta(\eta_o)]G(\eta,\eta_o)\,d\eta_o = \{BC\} + \int_{\eta_o=0}^{1} L_o^*[G(\eta,\eta_o)]\theta(\eta_o)\,d\eta_o \tag{11b}$$

where $G(\eta,\eta_o)$ is the appropriate Green's function and whose arguments are written to represent the (effect, cause) relationship. The conjunct in Eq. (11b) is denoted by the boundary conditions (BC), and L_o^* is the formal adjoint operator associated with the differential operator L_o. In order to emphasize that the integral is over the cause variable η_o, we have subscripted the differential operator L.

Formally, we proceed to integrate the left-hand side of Eq. (11b) by parts twice. Doing so yields

$$\int_{\eta_o=0}^{1} G(\eta,\eta_o)f(\eta_o,\theta,Q_o)\,d\eta_o = \left\{G(\eta,\eta_o)\frac{d\theta}{d\eta_o} - \theta(\eta_o) \times \frac{dG}{d\eta_o}(\eta,\eta_o)\right\}_{\eta_o=0}^{1} + \int_{\eta_o=0}^{1} L_o^*[G(\eta,\eta_o)]\theta(\eta_o)\,d\eta_o \tag{12a}$$

since $L_o[\theta(\eta_o)] = f(\eta_o,\theta,Q_o)$. Performing the indicated integrations in Eq. (12a), we find $L_o^* = L_o$; that is, L_o is formally self adjoint. From knowledge of the known boundary conditions, we will require

$$L_o^*[G(\eta,\eta_o)] = \delta(\eta_o - \eta)$$
$$G(\eta,0) = \frac{dG(\eta,1)}{d\eta_o} = 0 \tag{12b}$$

where $\delta(\eta_o - \eta)$ is the Dirac delta function. It is apparent that the Green's function can be interpreted as the response to a concentrated source at $\eta_o = \eta$ and subject to the homogeneous boundary condition imposed by Eq. (12b). Therefore we obtain the following integral equation

$$\theta(\eta) = -G(\eta,1)\frac{d\theta(1)}{d\eta_o} - \frac{dG(\eta,0)}{d\eta_o}\theta(0) + \int_{\eta_o=0}^{1} G(\eta,\eta_o)f(\eta_o,\theta,Q_o)\,d\eta_o \tag{12c}$$

It is readily seen that $G(\eta,\eta_o)$ is the kernel of the integral operator that inverts L_o. Solving Eq. (12b) by standard methods yields the two part Green's function

$$G(\eta,\eta_o) = \begin{cases} -\eta_o & 0 \le \eta_o \le \eta \\ -\eta & \eta \le \eta_o \le 1 \end{cases} \tag{12d}$$

Substituting the boundary conditions and $f(\eta_o,\theta,Q_o)$ into Eq. (12c) and performing some manipulations, we find

$$\sum_{m=0}^{MMAX} \frac{\beta_m^*}{(m+1)}\theta^{m+1}(\eta) = \sum_{m=0}^{MMAX} \frac{\beta_m^*}{(m+1)}\theta^{m+1}(0) + \eta\sum_{m=0}^{MMAX} \frac{\beta_m^*}{(m+1)}\frac{d\theta^{m+1}(1)}{d\eta_o} - N_r\int_{\eta_o=0}^{\eta} \eta_o\left[Q_o(\eta_o) - \frac{B^2}{2}\int_{\xi=0}^{1} \frac{Q_o(\xi)\,d\xi}{[B^2+(\xi-\eta_o)^2]^{3/2}} - \frac{1}{2\varepsilon}\left(1-\frac{\eta_o}{(B^2+\eta_o^2)^{1/2}}\right)\right]d\eta_o - N_r\int_{\eta_o=\eta}^{1} \eta\left[Q_o(\eta_o) - \frac{B^2}{2}\int_{\xi=0}^{1} \frac{Q_o(\xi)\,d\xi}{[B^2+(\xi-\eta_o)^2]^{3/2}} - \frac{1}{2\varepsilon}\left(1-\frac{\eta_o}{(B^2+\eta_o^2)^{1/2}}\right)\right]d\eta_o \tag{13a}$$

where $\beta_o^* \equiv 1$. Observe that an integral equation approach automatically incorporates the boundary conditions. That is, we may substitute the right-hand-side of Eq. (10a) for $\theta^{m+1}(0)$ and use Eq. (10b) to replace

$$\sum_{m=0}^{MMAX} \frac{\beta_m^*}{(m+1)}\frac{d\theta^{m+1}(1)}{d\eta_o} \tag{13b}$$

by $-\tau N_r\theta^4(1)$ when boundary is radiating. When the surface at $\eta_o = 1$ is insulated, the term represented in Eq. (13b) is replaced by zero in Eq. (13a). Finally, interchanging the orders of integration on the double integrals yields

$$\sum_{m=0}^{MMAX} \frac{\beta_m^*}{(m+1)}\theta^{m+1}(\eta) = \sum_{m=0}^{MMAX} \frac{\beta_m^*}{(m+1)}\theta^{m+1}(0) + \eta\sum_{m=0}^{MMAX} \frac{\beta_m^*}{(m+1)}\frac{d\theta^{m+1}(1)}{d\eta_o} - N_r\int_{\eta_o=0}^{\eta} \eta_o Q_o(\eta_o)\,d\eta_o - N_r\int_{\eta_o=\eta}^{1} \eta Q_o(\eta_o)\,d\eta_o + \frac{N_r B^2}{2}\int_{\xi=0}^{1} Q_0(\xi) \times [I_1(\xi,\eta) + I_2(\xi,\eta)]\,d\xi + \frac{N_r}{2\varepsilon}[I_3(\eta) + I_4(\eta)] \tag{14a}$$

where

$$I_1(\xi,\eta) = \int_{\eta_o=0}^{\eta} \frac{\eta_o \, d\eta_o}{[B^2 + (\xi - \eta_o)^2]^{3/2}} \tag{14b}$$

$$I_2(\xi,\eta) = \int_{\eta_o=\eta}^{1} \frac{\eta \, d\eta_o}{[B^2 + (\xi - \eta_o)^2]^{3/2}} \tag{14c}$$

$$I_3(\eta) = \int_{\eta_o=0}^{\eta} \eta_o \left(1 - \frac{\eta_o}{(B^2 + \eta_o^2)^{1/2}}\right) d\eta_o \tag{14d}$$

$$I_4(\eta) = \int_{\eta_o=\eta}^{1} \eta \left(1 - \frac{\eta_o}{(B^2 + \eta_o^2)^{1/2}}\right) d\eta_o \tag{14e}$$

In general, these well-behaved integrals may be easily evaluated by any numerical quadrature. In this case, these integrals may be evaluated analytically.[13] Next, we shall present numerical results that use the dual integral equation formulation as represented by Eqs. (9) and (14). In addition, a discussion of the simple numerical procedure will be outlined.

Results and Discussion

In this section, we present numerical results using the dual integral equation formulation. For convenience, but without loss of generality, we have assumed a linear variation in the thermal conductivity, namely $MMAX = 1$. A parametric study was undertaken to study the effects and ramifications of the various parameters. Equations (9) and (14) were discretized using the trapezoidal method having a global truncation error of $O(\Delta\eta^2)$.[14] A higher order block-by-block method using Simpson's rule with internal quadratic interpolations could have been incorporated. The global truncation error associated with this scheme would be $O(\Delta\eta^4)$.[17] The Gauss-Seidel underrelaxation method was the iterative scheme used.[15] The underrelaxation constant ω ranged between $0.4 < \omega < 0.7$ depending on N_r (a high N_r required a low ω). Finally, it should be mentioned that this formulation and solution methodology can be easily applied to fins of other profiles.

The authors wrote independent computer programs in Fortran IV and Fortran 77 that were executed on different machines (IBM XT with a 8087 coprocessor and a VAX 11/780, respectively). Typical run times using a VAX 11/780 are presented in Table 1, whereas the IBM PC-XT simulation typically required from 20 to 25 s. Identical numerical results were obtained and in agreement with the number of places presented in Table 2. In general, the computer codes required to generate the results consisted of 100–125 executable statements. These codes were not optimized for speed or redundancy in calculations.

As a comparison, a finite difference solution was developed for the single integro-differential equation formulation.[7] The single integro-differential equation in temperature is considered the standard formulation by which we can compare our methodology for accuracy, stability, speed, and ease of programming. The length of the program required for the finite difference simulation is comparable to the dual integral equation solution.

Some additional remarks must be stated before discussing and assessing the simulations. First, in general, program run times for the same problem varied depending on the programmer. Second, the finite difference solution was inherently less stable than the quadrature scheme used to resolve the coupled nonlinear integral equations. Finally, less finesse was required by the programmer in discretizing the system of nonlinear integral equations than was required in differencing the single integro-differential equation in temperature.[7]

Table 1 presents typical run times using the proposed dual integral equation approach. In order to demonstrate the potential of this method, a finite difference solution to the standard single integro-differential equation in temperature[7] was developed. The finite difference solution had inherent difficulties in stability, convergence, consistency of maintaining truncation errors, and programming. In order to obtain accurate results, a tolerance of 0.0001 was required. The typical number of iterations, when $\Delta\eta = 0.10$, was 327 while run times exceeded 1200 ms. If the step size was reduced to $\Delta\eta = 0.05$, the number of iterations exceeded 1600 while the run times surpassed 19,000 ms.

It is apparent that the new formulation and proposed solution methodology is superior for several reasons. First, convergence to the correct values using the dual integral equation approach is more rapid than the numerical solution of the integro-differential equation.[7] Second, control of truncation errors can be easily maintained by the proposed method. Third, the dual integral equation method is easy to program. Finally, the dual integral equation approach permits accurate results to be obtained rapidly and is apparently less sensitive to step size and tolerance than the finite difference solution of the single integro-differential equation.

Table 2 displays the temperature distribution corresponding to the cases presented in Table 1. These results demonstrate the accuracy available to the trapezoidal rule integration for a fixed tolerance. As can be seen by this table, an accurate solution may be obtained even with a course discretization. This table qualitatively displays the error associated with the integration scheme for fixed spatial step.

Next, we present results of the parametric study using the fin configuration shown in Fig. 1. For the sake of simplicity, the boundary condition at the open end of each fin is assumed to be insulated, thereby simplifying Eq. (10b). This study will display the temperature and radiosity distributions associated with the various parameters. The net amount of heat transfer can be obtained through conduction considerations or by calculating the net radiative loss.

Attention is first directed to the temperature and radiosity distributions as a function of the surface emissivity and radiation-conduction number N_r for fixed fin spacing $B = 1$. Figure 2 shows the temperature distribution for various emissivities and radiation-conduction numbers. It appears that the temperature distribution is weakly dependent on the emissivity for various radiation numbers[7] (note definition of N_r). Also, as the

Table 1 Typical number of iterations (Iter) for a given tolerance (Tol) for the temperatures and radiosities ($\beta_1^* = 0$) when a step size of $\Delta\eta$ is used in the trapezoidal rule integration[a]

Case	$\Delta\eta$	Tol	Iter	CPU time VAX 11/780, ms
1a	0.100	0.010	5	90.0
1b	0.050	0.010	5	339.0
2a	0.100	0.001	7	136.0
2b	0.050	0.001	7	505.0

[a] $\omega = 0.7$, $N_r = 1$, $B = 1$, $\varepsilon = 1$.

Table 2 Temperature distribution for different discretized spatial steps and tolerances used in trapezoidal rule integration corresponding to Table 1

Dimensionless position, η	Temperature, $\theta(\eta)$			
	Case 1a[a]	Case 1b[b]	Case 2a[c]	Case 2b[d]
0.00	1.0000	1.0000	1.0000	1.0000
0.10	0.9840	0.9839	0.9840	0.9839
0.20	0.9698	0.9696	0.9697	0.9696
0.30	0.9570	0.9569	0.9569	0.9569
0.40	0.9457	0.9456	0.9455	0.9455
0.50	0.9358	0.9356	0.9355	0.9354
0.60	0.9272	0.9271	0.9268	0.9267
0.70	0.9200	0.9200	0.9196	0.9196
0.80	0.9145	0.9146	0.9141	0.9141
0.90	0.9110	0.9112	0.9106	0.9105
1.00	0.9098	0.9100	0.9094	0.9093

[a] $\Delta\eta = 0.10$; tol = 0.01. [b] $\Delta\eta = 0.05$; tol = 0.01. [c] $\Delta\eta = 0.10$; tol = 0.001. [d] $\Delta\eta = 0.05$; tol = 0.001.

radiation-conduction number is increased, the temperature distribution becomes steeper. That is, for small N_r, conduction dominates and has a smoothing effect on the temperature distribution. In contrast, Fig. 3 shows that the corresponding radiosity distribution depends strongly on the radiation number and emissivity. Since a blackbody fin ($\varepsilon = 1$) has no reflected energy, the blackbody emissive power is the sole contributor to the outgoing radiation at any axial position in the fin. When a diffuse-gray surface having a emissivity of 0.6 is considered, the emissive power and a reflected component constitute the outgoing radiation. The combination of these appear to produce a radiosity distribution greater in magnitude than that associated with the blackbody case. Also, as the radiation number is decreased, the radiosity distribution grows larger in magnitude.

Next, consideration of the fin spacing B for various radiation-conduction numbers N_r is examined for a black surface ($\varepsilon = 1$). Figure 4 considers the effects of the fin spacing and radiation number on the temperature distribution. Again, it appears that for a black surface, the temperature distribution is weakly dependent on the fin spacing. The corresponding radiosity distributions are displayed in Fig. 5. The concavity of the radiosity distribution grows as the fin spacing is increased.

The variation in the temperature and radiosity distributions associated with a temperature dependent thermal conductivity is addressed Figs. 6–9. The standard linear variation in temperature is used; that is, Eq. (3) requires $MMAX = 1$ in order to get $k(T) = k_o(1 \pm \beta_1 T)$ where the reference temperature has been assumed at 0 K.

Figure 6 displays the temperature distributions associated with a blackbody fin having a spacing $B = 1$. A constant thermal conductivity, i.e., $k(T) = k_o$, has been omitted for sake of clarity in the drawings. However, this case is shown in Fig. 2 and can be superimposed on Fig. 6. It should be noted that a constant thermal conductivity will lie between the temperature distributions associated with $\pm\beta_1^*$ for fixed N_r. By reviewing Eqs. (8) and Fig. 6, one clearly sees that a positive β_1^* acts as an effective source while a negative β_1^* behaves as a sink. As the radiation number increases, the magnitude of the temperature distribution decreases. Figure 7 shows the corresponding radiosity distributions to Fig. 6. This figure shows that the radiosity distributions also appear to depend strongly on the radiation number and the thermal conductivity. A positive β_1^* (i.e., effective heat source) increases the local emissive power and thus increases the local radiosity.

Lastly, the effects of a diffuse-gray surface having an emissivity of 0.6 and temperature dependent thermal conductivity are considered for various radiation-conduction numbers. As mentioned previously, the effect of the emissivity, for the various radiation numbers, appears weak in determining the temperature distribution. This is also the case when a temperature

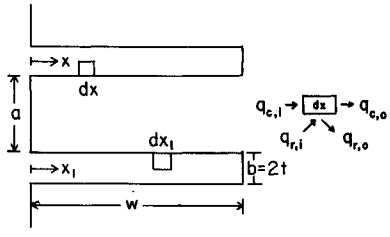

Fig. 1 Rectangular fin array with diffuse-gray surfaces having a common base temperature.

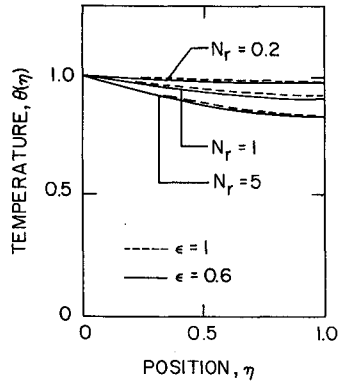

Fig. 2 Temperature distributions in fin considering constant thermal conductivity and B for various emissivities and radiation-conduction numbers N_r.

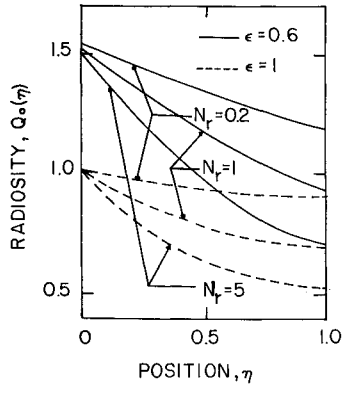

Fig. 3 Radiosity distributions associated with Fig. 2 for constant thermal conductivity and B for various emissivities and radiation-conduction numbers N_r.

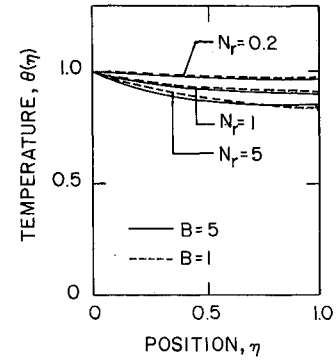

Fig. 4 Temperature distributions in fin considering constant thermal conductivity and $\varepsilon = 1$ for various radiation-conduction numbers N_r and fin spacings B.

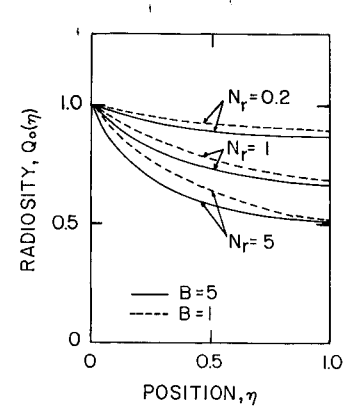

Fig. 5 Radiosity distributions associated with Fig. 4 for constant thermal conductivity and $\varepsilon = 1$ for various radiation-conduction numbers and fin spacings B.

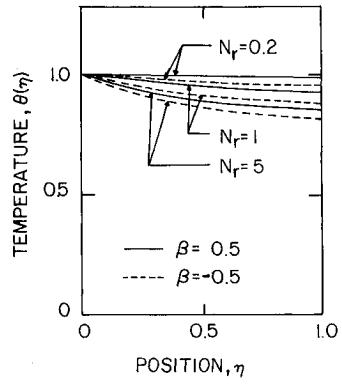

Fig. 6 Temperature distributions in fin considering $B = 1$ and $\varepsilon = 1$ for various radiation-conduction numbers N_r and a linear temperature variation in the thermal conductivity ($MMAX = 1$).

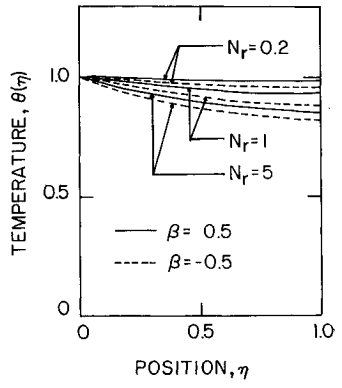

Fig. 8 Temperature distributions in fin considering $B = 1$ and $\varepsilon = 0.6$ for various radiation-conduction numbers N_r and a linear temperature variation in the thermal conductivity ($MMAX = 1$).

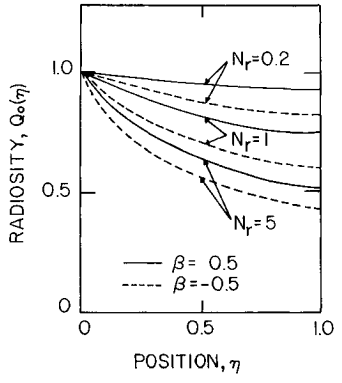

Fig. 7 Radiosity distributions associated with Fig. 6 for $B = 1$ and $\varepsilon = 1$ for various radiation-conduction numbers N_r and a linear temperature variation in the thermal conductivity ($MMAX = 1$).

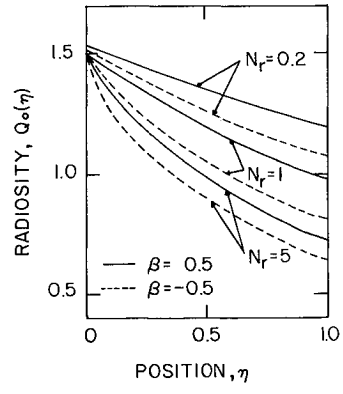

Fig. 9 Radiosity distributions associated with Fig. 8 for $B = 1$ and $\varepsilon = 0.6$ for various radiation-conduction numbers N_r and a linear temperature variation in the thermal conductivity ($MMAX = 1$).

dependent thermal conductivity is present. Again, the radiosity distribution appears to be strongly dependent on the emissivity and radition number. The radiosity distribution increases in magnitude significantly for decreasing emissivity, as seen by comparing Figs. 7 and 9.

The parametric study highlighted the temperature and radiosity distributions associated with the rectangular fin array under various conditions. The data required to generate the plots required a minimal amount of computer time and storage. The primitive or fundamental formulation only required a simple iterative scheme and numerical integration in which the error could be controlled. The solution methodology appears general and easy to program.

Conclusions

The present investigation demonstrates that the development of a primitive formulation used in conjunction with the Green's function method produces a natural analytic extension that leads to a direct and simple computational procedure. The proposed analytic-numeric solution methodology is demonstrated by considering a gray rectangular fin array[7] with a generalized temperature-dependent thermal conductivity. Through analytic manipulation presented by the Green's function method, two coupled nonlinear Fredholm integral equations are derived for the temperature and radiosity. The simultaneous numerical solution for the temperature and radiosity are carried out through a simple quadrature rule and a standard iteration scheme. The power of this formulation and subsequent computational procedure lies in the acquisition of accurate results obtained rapidly while being easy to program.

Tables 1 and 2 display typical run times and demonstrate the accuracy of the proposed methodology. Even with a course grid, accurate results are obtained. A finite difference code written for the single integro-differential equation[7] in temperature confirms the accuracy of the dual integral equation method. Unfortunately, the single integro-differential equation solution requires an excessive amount of computer time and has major stability constraints in order to produce accurate results. Therefore, the solution of the coupled nonlinear integral equations appears to be the solution method most applicable to conduction-radiation fin problems.

Though the rectangular fin profile is chosen to demonstrate the solution methodology, all common engineering fin profiles are amenable to the primitive formulation and subsequent computational procedure. Currently, an investigation of longitudinal fins is under way. This study addresses the design problem in detail since this type of fin configuration is more commonly used in space applications.

References

[1]Eslinger, R. G. and Chung, B. T. F., "Periodic Heat Transfer in Radiating and Convecting Fins or Fin Arrays," *AIAA Journal*, Vol. 17, Oct. 1979, pp. 1134–1140.

[2]Schnurr, N. M. and Cothran, C. A., "Radiation from an Array of Gray Circular Fins of Trapezoidal Profile," *AIAA Journal*, Vol. 12, Nov. 1974, pp. 1476–1480.

[3]Sparrow, E. M., Eckert, E. R. G., and Irvine, T. F., "The Effectiveness of Radiating Fins with Mutual Irradiation," *Journal of the Aerospace Sciences*, Vol. 28, Oct. 1961, pp. 763–772.

[4]Sparrow, E. M. and Eckert, E. R. G., "Radiant Interaction Between Fin and Base Surfaces," *Journal of Heat Transfer*, Vol. 84, Feb. 1962, pp. 12–18.

[5]Sparrow, E. M., Miller, G. B., And Jonsson, V. K., "Radiating Effectiveness of Annular-Finned Space Radiator, Including Mutual Irradiation Between Radiator Elements," *Journal of the Aerospace Sciences*, Vol. 29, Nov. 1962, pp. 1291–1299.

[6]Frankel, J. I. and Vick, B., "An Exact Methodology for Solving Non-linear Diffusion Equations Based on Integral Transforms," *Applied Numerical Mathematics*, Vol. 3, 1987, pp. 467–477.

[7]Siegel, R. and Howell, J. R., *Thermal Radiation Heat Transfer*, 2nd ed., McGraw-Hill, New York, 1981, pp. 393–395.

[8]Sparrow, E. M. and Cess, R. D., *Radiation Heat Transfer*, McGraw-Hill, New York, 1978.

[9]Roach, G. F., *Green's Functions*, 2nd ed., Cambridge Univ. Press, London, 1982, pp. 1–8.

[10]Greenberg, M. D., *Application of Green's Functions in Science and Engineering*, Prentice-Hall, Englewood Cliffs, NJ, 1971.

[11]Golberg, M. A. (ed.), *Solution Methods for Integral Equations*, Plenum, New York, 1979.

[12]Frankel, J. I., Vick, B., and Ozisik, M. N., "Flux Formulation of Hyperbolic Heat Conduction," *Journal of Applied Physics.*, Vol. 58, Nov. 1985, pp. 3340–3345.

[13]Beyer, W. H., (ed.), *CRC Standard Mathematical Tables*, 25th ed., Chemical Rubber Company, West Palm Beach, FL, 1978, pp. 345–347.

[14]Linz, P., *Analytical and Numerical Methods for Volterra Equations*, Society for Industrial and Applied Mathematics, Philadelphia, PA, 1985.

[15]Burden, R. L., Faires, J. D., and Reynolds, A. C., *Numerical Analysis*, 2nd ed., Prindle, Weber and Schmidt, Boston, MA, 1981, pp. 386–391.